Sustainable Futures 10 (2025) 100764

Contents lists available at ScienceDirect

Sustainable Futures

journal homepage: www.sciencedirect.com/journal/sustainable-futures

ENSO unleashed: Decoding energy consumption patterns across Nations

Alireza Olfati, Meysam Rafei [1,*], Siab Mamipour

Faculty of Economics, Kharazmi University, Tehran, Iran

ARTICLE INFO

Keywords:
El Niño
La Niña
Energy consumption per capita
Global vector autoregressive (GVAR) model

ABSTRACT

The intricate relationship between climate and energy consumption significantly impacts global sustainability and resilience. In this study, we address the critical gap in comprehensive research by examining the impact of El Niño and La Niña events on energy consumption across diverse nations. Our dynamic framework integrates 26 country/region-specific models estimated from historical data spanning 1979Q2 to 2023Q3. Employing the Global Vector Autoregressive (GVAR) model, we analyze the dynamic responses of energy consumption to El Niño Southern Oscillation (ENSO) shocks, accounting for regional variations. During ENSO episodes, discernible patterns emerge: El Niño leads to increased energy consumption in countries such as Australia, Indonesia, Malaysia, China, Japan, USA, and Saudi Arabia, while Argentina, Brazil, Chile, India, Mexico, and South Africa experience reduced energy consumption due to La Niña. The European region shows negligible effects. Our findings have direct implications for policymakers and energy stakeholders, emphasizing the importance of informed decision-making during ENSO events. Economic, environmental, and energy security challenges underscore the need for proactive measures.

1. Introduction

The impact of climate change on global variables is undeniable [5, 43], and among the most significant climate phenomena are El Niño and La Niña, collectively known as ENSO (El Niño Southern Oscillation) [27, 31]. The Pacific Ocean is far from tranquil; it was the fishermen in South America who first noticed this phenomenon in the 1600s upon encountering unusually warm waters in the Pacific Ocean. They referred to it as 'El Niño de Navidad,' owing to the tendency of El Niño to peak around December [17]. As depicted in Fig. 1., El Niño manifests when atmospheric pressure declines along South America's coast, leading to weakened trade winds and facilitating the eastward movement of warm water. This perturbation significantly impacts the normal upwelling process. Conversely, La Niña emerges when these conditions reverse, intensifying trade winds and enhancing upwelling [7]. Severe El Niño events were particularly notable in the years 1982–83, 1997–98, and 2015–16, while significant La Niña events occurred in 1988–89, 1998–99, and 2021–22, profoundly affecting global weather patterns and ecosystems[2] [2,20].

An extensive corpus of research has been dedicated to exploring the nexus between climatic conditions and various indicators of economic performance. This area of study is well-documented in the comprehensive surveys by Tol [37] and Dell et al. [12]. Historical and economic analyses have posited that the El Niño phenomenon could have been a contributing factor to a significant number of civil conflicts, as detailed in the study by Hsiang et al. [21]. However, studies investigating the impact of El Niño on energy consumption are scarce. El Niño impacts energy usage in the US. Natural gas consumption decreases in the Northwestern US, while nuclear electricity consumption is affected nationally. Hydroelectric power generation in the Southeastern US remains uncertain during El Niño [10]. This study by Thakker and Teegavarapu [35] assesses ENSO's impact on South Florida's climate and residential energy use, revealing significant temperature and consumption shifts during ENSO cycles, and aiding local energy planning.

Existing literature lacks a comprehensive analysis of the effects of ENSO on global energy consumption, with studies primarily focusing on national or regional impacts using methods that lack robustness. Our research fills this gap by employing a dynamic multi-country Global

* Corresponding author.
E-mail addresses: alirezaolfati@khu.ac.ir (A. Olfati), m.rafei@khu.ac.ir (M. Rafei), s.mamipoor@khu.ac.ir (S. Mamipour).
[1] Permanent address: Kharazmi University: No.43.Taleghani Ave, Tehran, Postal Code: 15,719–14,911, I.R. Iran

[2] Fig. 2. The side-by-side maps illustrate contrasting effects during El Niño and La Niña events. El Niño (left map) exhibits warmer sea surface temperatures (reds and oranges) primarily in the equatorial Pacific, while La Niña (right map) displays cooler anomalies (blues) in the same region. These thermal variations significantly influence marine ecosystems.

https://doi.org/10.1016/j.sftr.2025.100764
Received 25 July 2024; Received in revised form 8 January 2025; Accepted 30 May 2025
Available online 1 June 2025

Vector Autoregression (GVAR) model. This innovative approach combines time series, panel data, and factor analysis techniques to analyze the transmission of energy pattern changes resulting from El Niño shocks at both national and international levels [7]. It uniquely accounts for economic interdependencies and spillover effects across regions, while effectively isolating the ENSO shock from other potential sources of omitted variable bias. We enhance the climate-energy discourse by leveraging the exogenous variability in meteorological events, particularly focusing on ENSO, across time. This study assesses their influence on 26 country/region-specific models from 1979Q2 to 2023Q3. Our objective is to causatively delineate the impact of ENSO-induced meteorological disturbances on primary energy consumption per capita. In assessing the intensity of ENSO, our study employs the Bivariate EnSO Time series, BEST ENSO Index. To enhance the precision, detail, and robustness of our findings, we have disaggregated the BEST ENSO Index into its positive (El Niño) and negative (La Niña) phases. We then independently examined the relationship between the El Niño phase, temperature changes, and primary energy consumption per capita for each country/region, as well as for the La Niña phase. This analysis yielded intriguing results that corroborate our findings derived from the GVAR model and impulse response functions, which are discussed in detail in the results section of this paper.

In summary, our investigation into the impacts of ENSO on primary energy consumption per capita is pivotal for several reasons. Firstly, it provides a granular understanding of how global climatic oscillations influence energy consumption, a key determinant of economic stability and growth. Secondly, by employing a GVAR model, our study offers a robust analytical framework that captures the intricate interplay between climatic events and energy usage across multiple countries and regions. This approach not only enhances the precision of our findings but also contributes a novel methodology to the climate-energy literature. Lastly, the insights garnered from our research are instrumental for policymakers and energy sector stakeholders, enabling them to devise more informed and effective strategies to mitigate the economic repercussions of ENSO events. The urgency of addressing these climatic phenomena is underscored by their increasing frequency and intensity, as evidenced by Capotondi et al. [6] and Timmermann et al. [36]. These phenomena are likely to pose significant challenges to energy sustainability and economic resilience in the coming decades.

2. Literature review

While there is a wealth of research in this field, the objective of this section is not to comprehensively review the existing literature but rather to emphasize the primary conclusions derived from these studies. In essence, this research can be classified into three distinct clusters (see Table 1)

The first cluster comprises studies that investigate the impacts of El Niño on climatic and environmental conditions. A substantial body of literature has been dedicated to examining the effects of climate change, particularly focusing on the El Niño-Southern Oscillation (ENSO). Recent research has expanded the understanding of ENSO, showing its widespread impacts across Europe, Africa, Asia, and North America, affecting regions during extreme and "neutral" years [24]. ENSO's influence in South America leads to floods in Ecuador, Peru, and Colombia during El Niño and droughts in the Amazon and northeastern regions [3]. El Niño events, classified as EP (Eastern Pacific), MP (Mixed-type Pacific), and CP (Central Pacific), not only impact East Asian summer rainfall but also drive unique atmospheric circulation anomalies shaping regional precipitation patterns [22,41,45]. Additionally, recent studies have emphasized El Niño's role in increasing landslide risks in disaster-prone areas like Southeast Asia and Latin America, with satellite rainfall data integration and global landslide exposure models proving essential in showcasing the correlation between El Niño intensity and landslide occurrences [14]. Moreover, Yang et al. [44] review the evolving response of ENSO to global warming, addressing traditional dynamics, nuanced impacts with rising temperatures, challenges from Central Pacific El Niño events, and the influence on global teleconnection patterns and climate systems.

The relationship between ENSO, macroeconomics, and agriculture is investigated by researchers in the second group of studies, with a focus on the economic impacts of severe El Niño events in the context of climate change. A recent study finds that extreme El Niño events cause substantial global economic losses, while La Niña events result in minimal gains. Climate change worsens El Niño's impact, projecting trillions of dollars in losses by the 21st century's end [26]. A study by Cashin et al. [7] reveals that El Niño events trigger heterogeneous economic responses across countries. While Australia and India experience temporary downturns, the United States sees unexpected growth. However,

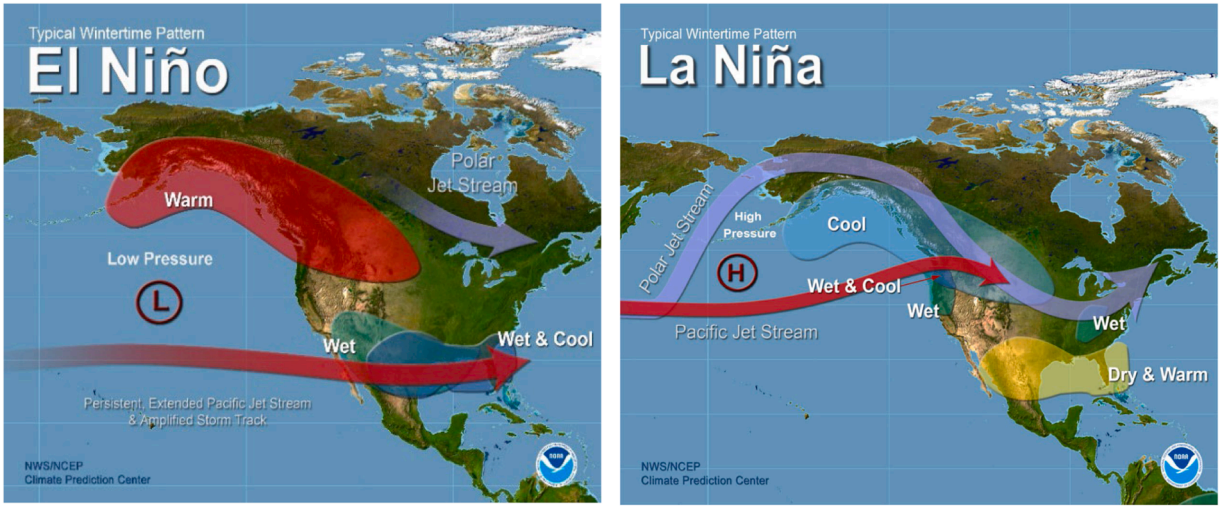

Fig. 1. Global climatological effects of ENSO.
Source: National Atmospheric and Oceanic Administration's (NOAA) Climate Prediction Center.

[3] Current research

short-term inflationary pressures are common due to energy and non-fuel commodity price surges. Zhang et al. [47] highlight the influence of El Niño on the Green Economy Index, emphasizing the need for policies supporting sustainable energy initiatives and addressing climate change risks. Furthermore, research shows that El Niño affects real equity returns across economies, with positive impacts during El Niño and negative impacts during La Niña [16]. El Niño-related inflation and disaster risks can be mitigated using silver as a hedge [32], while maize yields are significantly diminished by El Niño, particularly in lower-income, weather-vulnerable countries [38]. Effective monitoring and prediction are crucial for managing the socio-economic consequences of ENSO on the global wheat market, especially during La Niña events [19].

The third group of studies investigates the effects of ENSO on energy consumption. Although the literature on this topic is limited, existing studies primarily examine the relationship between GDP, carbon emissions, and energy use. Notably, Antonakakis et al. [1] reveal varied effects across income levels, a two-way causality between growth and energy use, and questions the efficacy of renewable energy for sustainable growth. Additionally, investigations highlight El Niño's multifaceted influence on energy consumption in the United States [10], the impact of La Niña on the EU's renewable energy stock market [40], and the interconnectedness between climate change, carbon emission trading, crude oil, and renewable energy markets [39]. These findings emphasize the need for climate risk management and timely decision-making by stakeholders. Furthermore, research in South Florida identifies significant fluctuations in temperature and energy consumption correlated with different ENSO phases, while another study shows ENSO as a predictor of WTI oil returns and volatility in financial markets and commodities [35].

However, a notable gap persists in the existing literature: there is a lack of a comprehensive study that examines the impacts of ENSO on global energy consumption. Previous research has often focused on regional analyses or specific sectors, leaving a void in our understanding of ENSO's worldwide energy implications. our research aims to bridge this gap by employing a GVAR model, which is particularly adept at capturing the complex interdependencies and dynamic interactions across national borders. This approach allows for a more nuanced understanding of how ENSO-related climatic variations influence energy consumption patterns on a global scale. By doing so, this study not only contributes to the academic discourse but also provides valuable insights for policymakers and energy economists in devising more resilient and adaptive energy strategies in the face of climate variability.

3. Modeling the climate–energy relationship in a global context

The Global Vector Autoregressive (GVAR) model stands out as the superior approach for climate-energy research due to its holistic analysis capabilities, accommodating both temporal and cross-sectional data dimensions. It adeptly captures the intricate interdependencies and spillover effects across nations, essential for evaluating the global impact of climate events on energy consumption. Additionally, the GVAR model's inclusion of unobserved common factors, such as commodity prices, enhances its analytical robustness. Its suitability for long-term relationship modeling and policy simulation further underscores its utility in addressing the complex dynamics of climate change and energy economics within a unified, theoretically sound framework. Before delving into the dataset and delineating our model's specifications, we provide an overview of the GVAR methodology.

3.1. The global VAR (GVAR) methodology

Our analysis examines the global economy by considering a total of $N + 1$ countries, denoted by the index i, which ranges from 0 to N. The United States is designated as the reference country with the index 0, while the remaining N countries are characterized as small open economies. Utilizing individual *VARX** models for each country, we construct the overarching GVAR framework. In line with the methodologies established by Pesaran [28] and Dees et al. [11], the $VARX^*(p_i, q_i)$ model for the ith country correlates $k_i \times 1$ vector of domestic macroeconomic variables, considered endogenous and denoted by $\boldsymbol{x}_{it}$, with a $k_i^* \times 1$ vector of country-specific foreign variables, deemed weakly exogenous, represented by x_{it}^*:

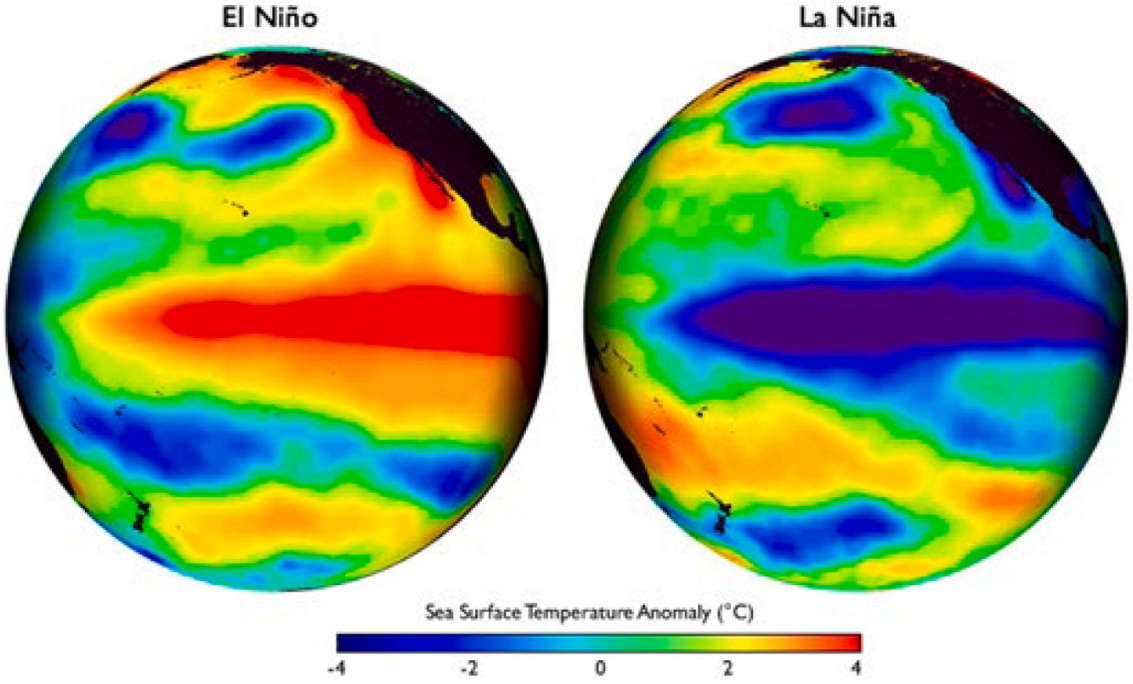

Fig. 2. Global impacts of El Niño and La Niña on sea surface temperature anomalies.
Source: National Atmospheric and Oceanic Administration's (NOAA) Climate Prediction Center.

Table 1
Recent research in brief[3].

cluster	Authors	Countries/Regions	Period	Data	methodology
ENSO And Climatic, environmental conditions	Lin and Qian [24]	Globally	1880–2016	Extended Reconstructed Sea Surface Temperature (ERSST), Climatic Research Unit Time-Series (CRUTS), Global Precipitation Climatology Center (GPCC)	Two-tier Approach
	Cai, McPhaden, Grimm, Rodrigues, Taschetto, Garreaud, Dewitte, Poveda, Ham, et al. [4]	South American continent	19th - 2010s	Southern Oscillation Index (SOI)	Synthesis Approach
	Wen et al. [41]	East Asian	1958 - 2015	Monthly precipitation (PREC), monthly surface skin temperature (SKT), and Niño 3.4	Synthetic Analysis Method
	R. Emberson et al. [15]	Globally	2000–2019	New Satellite Rainfall, Global Landslide Exposure	Empirical Analysis
	Yang et al. [44]	Globally	20th-21th	Niño 3.4	Synthesis Review
ENSO And economic	Liu et al. [26]	Globally	1960–2019	Niño 3.4, SST, Land-Based Air Surface Temperature, GDP	OLS
	Cashin et al. [7]	Globally	1979–2013	Niño 3.4, GDP, inflation, Energy and non-fuel commodity price	GVAR
	Zhang et al. [47]	Globally	2010–2022	SOI, NASDAQ OMX Green Economy Index	GARCH-MIDAS
	Ginn [16]	20 Countries	2000–2023	Niño 3.4, GDP, Aggregate CPI, Equity price, Interest Rate	Panel Local Projections (panel LP)
	Salisu et al. [32]	Globally (33 Countries)	1980–2019	SOI, GDP, Inflation, Short-Term Interest rate, Long-Term Interest rate, Exchange rate, Equity price, Commodity price	GVAR
	Ubilava and Abdolrahimi [38]	Globally (67 Countries)	1961–2017	Sea Surface Temperature (SST), Maize Yields	OLS
	Gutierrez [19]	USA-ARG-AUS-CAN-RUK-EU-ROW (Rest Of the World)	2000–2016	Niño 3.4, Wheat Export Price, Wheat Stock to Use Ratio, Nominal Exchange Rate, Fertilizer Price	GVAR
ENSO And energy consumption	Antonakakis et al. [1]	Globally (106 countries)	1971–2011	GDP, Energy Consumption, Carbon Dioxide Emissions	PVAR
	Collins [10]	USA	1970–2000	Niño 3.4, Energy Consumption (coal, natural gas, electricity)	spatial and statistical analysis
	Wei et al. [40]	Globally	2004–2021	Multivariate ENSO Index (MEI), the European Renewable Energy Total Return Index (ERIX), Wilder Hill Clean Energy Index (ECO)	Quantile
	Wei et al. [39]	Globally	2005–2021	Multivariate ENSO Index (MEI)-EU Allowance (EUA)- Brent oil prices- the Wilder Hill index	TVP-VAR
	Demirer et al. [13]	USA	1876–2021	Real West Texas Intermediate (WTI) oil price, SOI, Real Oil Price (ROILR)	Quantile

Note: *The RUK countries encompass Russia, Ukraine, and Kazakhstan.

$$\boldsymbol{\Phi_i}(\boldsymbol{L}.\boldsymbol{p_i})\boldsymbol{x_{it}} = \boldsymbol{a_{i0}} + \boldsymbol{a_{i1}}\boldsymbol{t} + \boldsymbol{\Lambda_i}(\boldsymbol{L}.\boldsymbol{q_i})\boldsymbol{x^*_{it}} + \boldsymbol{u_{it}} \quad (1)$$

$t = 1, 2, \ldots, T$, denotes the time. The terms $\boldsymbol{a_{i0}}$ and $\boldsymbol{a_{i1}}$ represent $k_i \times 1$ vectors that contain the fixed intercepts and the coefficients for the deterministic time trends, respectively. The term $\boldsymbol{u_{it}}$ is a $k_i \times 1$ vector representing idiosyncratic shocks specific to each country. These shocks are presumed to be independent and identically distributed with a zero mean and a distinct, non-degenerate covariance matrix Σ_{ii} denoted as $\boldsymbol{u_{it}} \sim$ i.i.d. $(0, \Sigma_{ii})$. For the sake of simplicity in algebra, we do not consider observed global factors within the individual country-specific $VARX^*$ models. Additionally, $\boldsymbol{\Phi_i}(L, p_i) = I - \sum_{i=1}^{p_i} \boldsymbol{\Phi_i} L^i$ and $\boldsymbol{\Lambda}(L, q_i) = \Sigma_i^{q_i} \boldsymbol{\Lambda_i} L^i$ represent the matrix lag polynomials of the coefficients linked to the domestic and international variables, respectively. The selection of the lag orders for the variables p_i and q_i is tailored individually for each country. This approach permits the distinct specification of $\boldsymbol{\Phi_i}(L, p_i)$ and $\boldsymbol{\Lambda}(L, q_i)$, thereby acknowledging that these parameters may vary among different nations. in constructing the foreign variables unique to each country, we take the domestic variables and compute their cross-sectional averages. These averages are determined by using the bilateral trade figures as weights, denoted by w_{ij}:

$$\boldsymbol{x^*_{it}} = \sum_{j=0}^{N} \boldsymbol{w_{ij}} \boldsymbol{x_{j_t}} \quad (2)$$

where j ranges from 0 to N, with w_{ii} set to 0 to avoid self-weighting, and the sum of the weights $\left(\sum_{j=0}^{N} w_{ij} = 1\right)$ to ensure a normalized average. In the empirical analysis, trade weights are derived by calculating the average over a three-year period. The formula is as follows:

$$\boldsymbol{w_{ij}} = \frac{\boldsymbol{Tij}, 2009 + \boldsymbol{Tij}, 2010 + \boldsymbol{Tij}, 2011}{\boldsymbol{Ti}, 2009 + \boldsymbol{Ti}, 2010 + \boldsymbol{Ti}, 2011} \quad (3)$$

where T_{ijt} represents the bilateral trade flow between country i and country j in year t, computed as the mean of country i 's exports to and imports from country j. The term T_{it} denotes the total trade of country i, which is the sum of bilateral trades T_{ijt} with all countries j for the years 2009, 2010, and 2011 $\left(T_{it} = \sum_{j=0}^{N} T_{ijt}\right)$.

While the estimation process is conducted individually for each country, the GVAR model is resolved globally, recognizing that all variables are inherently interdependent within the system. Following the separate estimation of each country's $VARX^*(p_i, q_i)$ model, it is necessary to solve for all $k = \sum_{i=0}^{N} k_i$ endogenous variables concurrently. These variables are aggregated into a $k_i \times 1$ vector x_t, which includes $(\boldsymbol{x'}_{0t}, \boldsymbol{x'}_{1t}, \ldots, \boldsymbol{x'}_{Nt})'$. This simultaneous resolution is facilitated by a link matrix, which is constructed based on weights specific to each country. To illustrate, the $VARX^*$ model presented in Eq. (1) can be succinctly expressed as:

$$\boldsymbol{A_i}(\boldsymbol{L}, \boldsymbol{p_i}, \boldsymbol{q_i})\boldsymbol{z_{it}} = \boldsymbol{\varphi_{it}} \quad (4)$$

for $i = 0, 1, \ldots, N$

$$\boldsymbol{A_i}(L, p_i, q_i) = [\Phi_i(L, p_i) - \Lambda_i(L, q_i)], \ \boldsymbol{z_{it}} = \left(\boldsymbol{x'}_{it}, \boldsymbol{x^{*'}_{it}}\right)',$$

$$\varphi_{it} = a_{i0} + a_{i1}t + u_{it} \tag{5}$$

Note that given Eq. (2). we can write:

$$z_{it} = W_i x_t \tag{6}$$

where $W_i = (W_{i0}, W_{i1}, \ldots, W_{iN})$, with $W_{ii} = 0$, is the $(k_i + k_i^*) \times k$ weight matrix for country i defined by the country-specific weights, wij_{ih}. Using Eq. (6) we can write Eq. (4) as:

$$A_i(L, p)W_i x_t = \varphi_{it} \tag{7}$$

$A_i(L, p)$ is constructed from $A_i(L, p_i, q_i)$ by setting $p = max(p_0, p_1, \ldots, p_N, q_0, q_1, \ldots, q_N)$ and augmenting the $p - p_i$ or $p - q_i$ additional terms in the power of the lag operator by zeros. Stacking Eq. (7) we obtain the Global VAR(p) model in domestic variables only:

$$G(L, p)x_t = \varphi_t \tag{8}$$

$$G(L, p) = \begin{pmatrix} A_0(L,p)w_0 \\ A_1(L,p)w_1 \\ \cdot \\ \cdot \\ \cdot \\ A_N(L,p)w_N \end{pmatrix}, \quad \varphi_t = \begin{pmatrix} \varphi 0t \\ \varphi 1t \\ \cdot \\ \cdot \\ \cdot \\ \varphi Nt \end{pmatrix} \tag{9}$$

An initial demonstration of the resolution process for the GVAR model, employing a $VARX^*(1, 1)$ structure, is documented in Pesaran [28]. For a comprehensive review encompassing recent advancements in GVAR modeling—spanning both its conceptual underpinnings and a wide array of empirical implementations—refer to the study by Chudik and Pesaran [9]. The GVAR(p) formulation, as delineated in Eq. (8), is amenable to recursive computation and serves various analytical functions, including forecasting and conducting impulse response assessments. Chudik and Pesaran [8] broadens the scope of the GVAR methodology by incorporating common variables into the conditional models specific to each country. These variables may manifest as either observable global factors or as dominant variables. Under these conditions, Eq. (1) necessitates enhancement through the inclusion of a vector comprising dominant variables, denoted as ω_t, along with its lagged counterparts.

$$\Phi_i(L, p_i)x_{it} = a_{i0} + a_{i1}t + \Lambda i(L, q_i)x_{it}^* + \Upsilon_i(L, s_i)\omega_t + u_{it} \tag{10}$$

Where $\Upsilon_i(L, s_i) = \sum_{i=0}^{S_i} \Upsilon_i L^i$ represents the matrix lag polynomial for the Type equation here.coefficients linked to the common variables, the variable ω_t may be regarded—and empirically verified—as weakly exogenous when estimating. The peripheral model concerning the dominant variables is estimable, irrespective of the feedback effect from x_t. To accommodate the feedback from the variables within the GVAR framework to the dominant variables through cross-sectional means, the subsequent model is posited for ω_t:

$$\omega_t = \sum_{I=1}^{p_w} \Phi_{\omega I}\omega_{i,t-1} + \sum_{I=1}^{p_w} \Lambda_{\omega I}x_{i,t-1}^* + \eta_{\omega t} \tag{11}$$

It is pertinent to observe that the simultaneous values of the star variables are absent in Eq. (1), rendering ω_t to be "causal". As previously elucidated, the conditional model delineated in Eq. (10) and the marginal model outlined in Eq. (11), can be amalgamated and resolved within the framework of a comprehensive GVAR model.

3.2. Model specification

Our model encompasses 33 countries, incorporating 26 country/region-specific models that collectively account for over 90 % of the world's GDP, as delineated in Table 3. We specify a series of individual country-specific models. These 26 $VARX^*$ models comprise seven domestic variables, contingent upon the availability of data for each variable.

$$x_{it} = \left[y_{it}, \pi_{it}, eq_{it}, r_{it}^s, r_{it}^L, ep_{it}, ECp_{C_{it}}\right]' \tag{12}$$

y_{it} represents the logarithm of the real Gross Domestic Product at time t for country i, π_{it} denotes inflation, eq_{it} is the logarithm of real equity prices, r_{it}^s and r_{it}^L are the short- and long-term interest rates respectively, ep_{it} is the real exchange rate and $ECp_{C_{it}}$ signifies energy consumption per capita, alternatively described as energy use per person. In addition, all domestic variables, except for that of the real exchange rate, have corresponding foreign variables computed as in Eq. (2):

$$x_{it}^* = \left[y_{it}^*, \pi_{it}^*, eq_{it}^*, r_{it}^{*s}, r_{it}^{*L}, ECpc_{it}^*\right]' \tag{13}$$

In consideration of our objective to examine the ramifications of ENSO shocks, it is imperative to incorporate the Bivariate ENSO Time Series (BEST) within our analytical structure. We posit BEST as a dominant variable, under the premise that it remains uninfluenced by the aforementioned variables. Consequently, BEST is integrated as a weakly exogenous factor across all 26 country/region-specific $VARX^*$ models, ensuring that the macroeconomic variables exert no reciprocal influence on BEST, thereby establishing a one-way causal relationship.

We sourced the six macroeconomic indicators for the 33 countries in our sample (refer to Table 2) from the GVAR Quarterly Dataset, as documented by Kamiar Mohaddes[4] and outlined in Smith and Galesi [34]. Data on energy consumption per capita (ECpc) were acquired from the 2022 edition of 'Energy use per person' at our World in Data website.[5] primary energy includes the energy required by end users for electricity, transportation, and heating, as well as accounting for inefficiencies and losses during the transformation of raw resources into usable forms. the Bivariate ENSO Time Series (BEST) Index was obtained

Table 2
Lag orders of the country-specific $VARX^*(p, q)$ models together with the number of cointegrating relations (r)[8].

	$VARX^*$ order		Cointegrating relations (r_i)		$VARX^*$ order		Cointegrating relations (r_i)
country	p_i	q_i		country	p_i	q_i	
Argentina	2	2	1	Norway	2	1	0
Australia	2	2	2	New Zealand	2	2	2
Brazil	2	2	1	Peru	2	2	2
Canada	2	1	1	Philippines	2	1	1
China	2	1	1	South Africa	2	2	1
Chile	2	2	2	Saudi Arabia	2	2	1
Europe*	2	1	1	Singapore	2	1	1
India	2	1	1	Sweden	2	2	0
Indonesia	2	1	2	Switzerland	2	1	1
Japan	2	2	1	Thailand	2	1	1
Korea	2	2	1	Turkey	2	2	1
Malaysia	2	1	1	United Kingdom	2	1	1
Mexico	2	1	1	USA	2	1	1

Notes: *Europe includes the following 8 countries: Austria, Belgium, Finland, France, Germany, Italy, Netherlands and Spain. The lag order for domestic and foreign variables, denoted as pi and qi respectively, is determined using the Akaike Information Criterion (AIC). The selection of cointegrating relations (r_i) relies on maximal eigenvalue test statistics, computed based on 95 % simulated critical values from stochastic simulations with 100 replications. However, for Sweden and Norway, we intentionally reduced (r_i) below the values suggested by the maximal eigenvalue statistic to ensure well-behaved persistence profiles.

[4] https://www.mohaddes.org/gvar.
[5] https://ourworldindata.org/grapher/per-capita-energy-use.

from the National Oceanic and Atmospheric Administration's National Climatic Data Centre.[6] This index[7] is designed for simplicity in computation and extends the temporal scope for research applications. Traditionally, the Niño 3.4 index has served as the standard for gauging ENSO's strength within the tropical Pacific. However, its solitary application overlooks critical atmospheric dynamics. The integration of the Southern Oscillation Index (SOI)—the barometric pressure differential between Tahiti and Darwin—addresses this gap by encapsulating atmospheric interactions more comprehensively. Furthermore, historical Sea Surface Temperature (SST) records, which are often partially reconstructed, introduce biases. The inclusion of the SOI, with its robust historical measurements, mitigates these biases, offering a more accurate representation of ENSO's influence [33]. Our analysis utilizes quarterly data spanning from 1979Q2 to 2023Q3 to estimate the 26 country-specific $VARX^*(pi,\ qi)$ models. Given that the dataset for ECpc extends only up to the year 2022 and is presented on an annual basis, we initially project the 2023 data utilizing the ARIMAX model. Subsequently, we transform the data's frequency to a quarterly scale employing the Litterman method [25]. This approach is renowned for its efficacy in frequency conversion from lower to higher intervals, ensuring minimal discrepancies in the data.

Fig. 3

Prior to estimation, we determined the optimal lag orders for domestic and foreign variables,p_i and q_i, using the Akaike Information Criterion (AIC) on the base unrestricted $VARX^*$ models. Due to data limitations, we imposed a maximum lag order of four ($p_{max} = q_{max} = 2$). The chosen orders for the $VARX^*$ models are detailed in Table 2. Additionally, the BEST model's lag order was set at one, based on the AIC.

Upon determining the lag order for the 26 $VARX^*$ models, our next step involves identifying the quantity of long-run relations. We employ cointegration examinations to test the null hypothesis, which ranges from the absence of cointegration to the presence of multiple cointegrating relationships. These tests are conducted in accordance with Johansen's maximal eigenvalue and trace statistics, as delineated in Pesaran et al. [30], which cater to models incorporating weakly exogenous $I(1)$ regressors, unrestricted intercepts, and restricted trend coefficients. The selection of cointegrating relations r_i is informed by the maximal eigenvalue test statistics, alongside the 95 % simulated critical values derived from stochastic simulations with 100 replications.

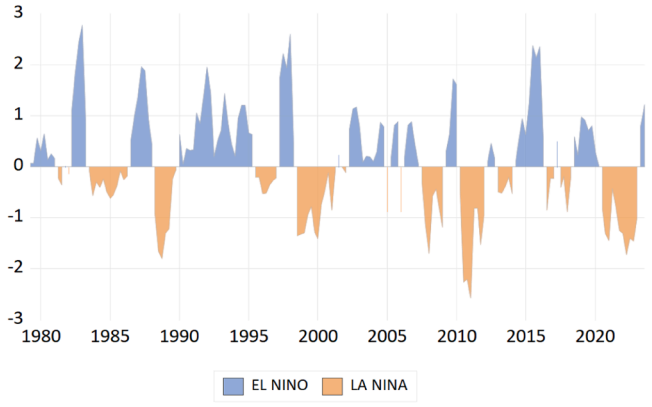

Fig. 3. Bivariate ENSO Time Series—The BEST ENSO Index from 1979Q2 to 2023Q3. Constructed by the authors using data from the U.S. National Oceanic and Atmospheric Administration's National Climatic Data Center.

[6] https://psl.noaa.gov/people/cathy.smith/best.

[7]

[8] Current research

Subsequently, we assess the repercussions of global shocks on the precisely delineated cointegrating vectors by employing persistence profiles as conceptualized by Lee and Pesaran [23] and further refined by Pesaran and Shin [29]. The initial normalization of these persistence profiles $(pp_s)$is set to one, serving as a benchmark. However, their gradual decline towards zero offers insights into the velocity of the equilibrium restoration process following shocks. Although the (pp_s) may initially surpass the benchmark, indicating an overshoot, they are required to converge to zero ultimately, confirming the cointegration of the vector in question. In the examination of the PPs, it was observed that convergence occurred at a notably sluggish pace for Sweden and Norway, with the latter exhibiting persistent system-wide shocks. Consequently, a value of zero was allocated for the parameter r_i for each nation, ensuring the (pp_s) behaved appropriately. Table 2 presents the definitive selection of the number of cointegrating relationships.

4. Empirical findings: ENSO's influence on per capita energy consumption

To delineate the dichotomous stages of the ENSO cycle, a dummy variable was constructed, assigned a value of one during positive (negative) phases of the BEST index and zero in all other instances. This dummy variable was then multiplied by the BEST index to derive a quantifier for the El Niño (La Niña) phase. The resultant BEST index, termed POSBEST and NEGBEST, were incorporated into the GVAR model as distinct series. These series were subjected to negative and positive one standard deviation shocks, respectively, to analyze the repercussions of El Niño and La Niña episodes on energy consumption per capita.

4.1. The El Niño effects

Fig. 4. presents the calculated median impulse responses of energy consumption per capita to an El Niño shock, inclusive of the 5 %–95 % lower and upper bootstrapped error bands. The responses are depicted at the initial impact and extend up to 40 quarters. The findings indicate that an El Niño occurrence exerts a statistically significant influence on the energy consumption per capita in numerous countries within our sample, as evidenced at the 5 %–95 % (blue short-dashed) levels. The summary of results is presented in Table 3 for each country.

In Argentina, an El Niño shock leads to a modest decrease in energy consumption per capita (ECpc), with the strongest effect observed two quarters after the shock (Fig. 4). Interestingly, the responses upon immediate impact and one quarter thereafter are not statistically significant. This is likely attributable to Argentina's generally mild winters, where a slight decrease in temperature does not significantly impact ECpc. Our impulse response functions (IRFs) reveal a decrease in real GDP following El Niño occurrences. We corroborate this finding by referencing Antonakakis et al. [1], who established a direct link between energy consumption and real GDP in upper-middle-income countries. However, our results diverge from Cashin et al. [7], who attributed Argentina's real GDP growth solely to increased soybean exports. While precisely quantifying El Niño's impact on real GDP remains challenging, we emphasize the critical role of the agriculture and livestock sectors, which are directly affected by El Niño-related weather anomalies. Additionally, El Niño disrupts rainfall patterns, influencing hydropower generation. Although increased rainfall can boost hydroelectric power production, extreme weather events associated with El Niño may lead to power outages and increased maintenance costs. Our findings reveal similarities across Brazil, Peru, and Argentina. However, Mexico experiences an initial decrease in energy consumption, which, although statistically insignificant, becomes significant at the 5 %−95 % level. Notably, Mexico's energy consumption stabilizes positively over a 10-year horizon, starting from the fifth quarter after the El Niño event. In Chile, El Niño disrupts electricity production from hydropower sources. Reduced output from hydropower dams and thermal plants necessitates

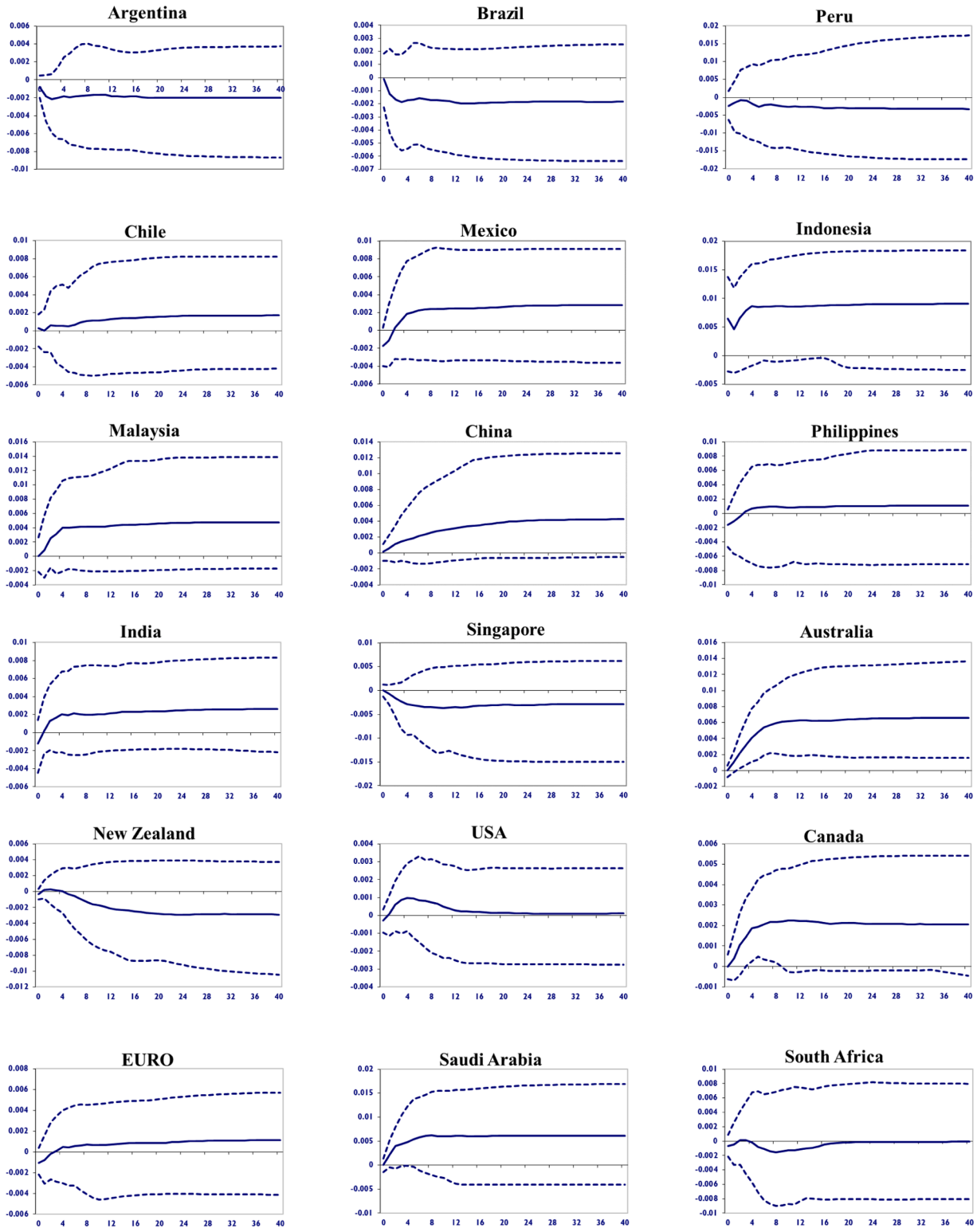

Fig. 4. The effects of an El Niño shock on energy consumption per capita. Notes: The figures represent the median impulse responses resulting from a one standard deviation negative shock to the positive component of BEST (POSBEST). These responses are accompanied by the 5 %–95 % error bands (indicated by blue short-dashed lines), and the analysis is conducted at a quarterly horizon.

increased reliance on fossil fuels (such as natural gas and oil) to offset the energy deficit. Consequently, consumers may face higher electricity costs during El Niño events due to supply constraints. Despite these challenges, Chile's trade partnerships with Europe, China, and USA play a compensatory role [7]. These economic ties boost Chile's GDP, mitigating the adverse effects of El Niño on energy consumption. Overall, the impact on energy consumption in Chile remains statistically insignificant. El Niño typically induces drier conditions over Southeast Asia, including Indonesia and Malaysia, especially during the boreal summer and fall [42]. Consequently, there is an increase in cooling demand energy, which corroborates the results of the impulse response function for Indonesia. As depicted in Fig. 4, the effect is significant at the 5 %–

Table 3
ENSO'S impact across the globe focusing on the energy sector.

Countries/ regions	El Niño	La Niña
Argentina	Milder winters, Reduction in heating demand (+)	Cooler summers (+)
Australia	Higher Temperature, increased Cooling Demand, energy requirements for agriculture and water Management (−)	milder summers in the Northern areas (+)
Brazil	High water levels in reservoirs, reduction in electricity rate (+)	Milder summers (+)
Canada	Colder winters, growth in real GDP (−?)	More rain and snow than average (+?)
China	Poor air quality, reduction in energy efficiency (−)	Increased Precipitation in Southern areas during Winter (+)
Chile	reduction in output from hydropower dams and thermal plants, more reliance on fossil fuel, higher temperatures (−?)	Lower temperature (+)
Europe*	Warmer and wetter winters in Southern European countries (+?)	(?)
India	Weaker monsoons, Rapid urbanization, fossil fuel consumption (?)	Above-normal rainfall in northwest Areas, enhanced air quality in northern India (+)
Indonesia	An uptick in dry days, reduced hydropower generation (−)	increased precipitation, reduction in heating demand (+)
Japan	Increased occurrences of typhoon strike (−)	Hotter summers and colder winters (−?)
Korea	Milder winters, Reduction in heating demand (+?)	(?)
Malaysia	Drier condition (−)	Above-average rainfall (+)
Mexico	Warmer weather (?)	Milder summer (+?)
Norway	(+?)	(−?)
New Zealand	Colder winters (−?)	More northeasterly winds, moist conditions in the northeast North Island, reduced rainfall in the south and southwest of the South Island, and higher temperature than normal (−)
Peru	Heavy rains in the north and east, Milder winter (+)	Reduction in Residential and commercial cooling demand (+)
Philippines	Reduced rainfall and cyclonic activity (?)	(?)
South Africa	Warmer and drier conditions (−?)	Above-average Rainfall, cooler summer temperatures (+)
Saudi Arabia	(−?)	Increased rainfall in the western parts (?)
Singapore	Transition to natural gas, solar panel installation, Carbon footprint reduction, Net-zero power pursuit (+)	Higher energy consumption for irrigation, processing, and transportation of agricultural products (−?)
Sweden	(+?)	(−?)
Switzerland	Warmer winters (+)	(−?)
Thailand	Drier condition (?)	Stronger monsoon rains, more energy demand (−)
Turkey	Warmer winters (+?)	(+?)
United Kingdom	(+?)	(−?)
USA	Colder winters, growth in real GDP (−?)	Colder Temperatures in the Northwest, dry conditions in the Southern States, higher Temperatures in the Southeast and Mid-Atlantic regions, increased Atlantic Hurricane activity (?)

Notes: *Europe includes the following 8 countries: Austria, Belgium, Finland, France, Germany, Italy, Netherlands and Spain. The symbols (+), (−), and (?) represent the positive, negative, and ambiguous effects of ENSO, respectively. Current Research: Compiled by the authors based on covariance analysis between temperature changes and the BEST index, as well as Impulse Response Functions analysis, in conjunction with relevant studies.

95 % level from one quarter after the shock until 10 years ahead. The most pronounced effect is observed in the fourth quarter after the shock (one year), after which it remains stable over 36 quarters. Notably, both China and Japan in East Asia exhibit similar responses, mirroring the behavior observed in Saudi Arabia within the Middle East. As established by Gong and Xu [18], a direct correlation exists between air quality and energy efficiency. Additionally, Zeng et al. [46] highlight that deteriorating air quality leads to increased reliance on indoor air purifiers, resulting in elevated energy consumption. Conversely, countries such as Korea, the Philippines, India, and Thailand experience an initial insignificant decrease in energy consumption approximately one year after the shock. However, their energy consumption subsequently stabilizes at positive levels for up to nine years ahead. Intriguingly, Singapore's impulse response function (IRF) reveals a significant decrease in energy consumption two years after the shock, eventually stabilizing at negative levels. However, the IRF does not exhibit significance within the first two quarters after the shock. Several factors may explain this phenomenon. First, Singapore has diligently implemented energy-efficient practices across various sectors, including efficient lighting, appliances, and industrial processes. Second, the nation's transition from fuel oil to natural gas for power generation has resulted in lower emissions and improved overall energy efficiency. Despite spatial constraints, Singapore has also embarked on installing solar panels atop high-rise buildings to harness solar energy, aiming to reduce reliance on conventional energy sources. Furthermore, Singapore's commitment to reducing its carbon footprint and addressing climate change impacts contributes to the observed decline in energy consumption. Given its low-lying geography, Singapore remains particularly susceptible to rising sea levels. Looking ahead, the pursuit of net-zero power by 2045 and plans to double renewable energy imports will further enhance energy security and sustainability.

From the Pacific region, it is evident that Australia experiences a significant increase in energy consumption per capita due to intensified cooling demands, higher temperatures, and elevated energy requirements for agriculture and water management during El Niño-induced drought conditions. Additionally, reduced hydroelectric power output prompts a shift toward alternative energy sources, further amplifying energy usage. In contrast, New Zealand's response diverges from Australia's expected pattern. Factors such as unique geography (New Zealand is surrounded by ocean, which moderates its climate. In contrast, Australia has vast arid regions and a different climate regime.), local climate drivers (including the Southern Annular Mode), reliance on renewable energy, and adaptive policies contribute to an insignificant IRF for energy consumption in New Zealand during El Niño shocks.

In USA, Collins [10] found that energy consumption tends to increase during El Niño events. Although this trend was not statistically significant overall, it was particularly pronounced in the context of nuclear electricity consumption. As depicted in Fig. 4, the initial El Niño shock is associated with a neutral IRF after one quarter. However, the IRF gradually increases, reaching a peak in the fourth quarter, before declining and eventually neutralizing after four years from the initial shock. Canada exhibits approximately the same response to El Niño events as the USA. However, an analysis of the correlation between POSBEST and temperature changes in both countries reveals milder winters, resulting in reduced heating requirements. Surprisingly, despite this winter trend, energy demand has increased. We posit that this rise is associated with the positive impact of El Niño events on their respective real GDPs.

In our model European region, which includes Austria, Belgium, Finland, France, Germany, Italy, The Netherlands, and Spain, energy consumption initially declined by one quarter following the shock. This reduction can be attributed to the impact of warmer and wetter winters in Southern European countries, specifically France, Italy, and Spain. However, approximately six quarters after the initial shock, energy consumption stabilizes at a positive level. This stabilization aligns with the overall GDP growth trend observed in European countries within our

region. Notably, Turkey exhibits a similar response pattern. Conversely, Northern countries such as the United Kingdom (UK), Norway, and Sweden demonstrate a consistent IRF. This persistent decline suggests a potential decoupling of energy consumption from economic growth in these regions. Switzerland, positioned as a central European country, shows a stable positive IRF. However, this effect becomes statistically insignificant within two quarters after the shock.

In the context of El Niño's climatic repercussions, South Africa's energy consumption per capita is susceptible to an uptick, primarily due to the warmer and drier conditions prevalent during such events. The literature delineates a clear trajectory of increased electricity demand for cooling purposes, intensified energy usage in agriculture due to escalated irrigation needs, and a potential pivot towards fossil fuels owing to diminished hydroelectric power generation. These factors collectively underscore the necessity for strategic energy planning and policy adaptation to mitigate the impacts of El Niño on South Africa's energy sector. However, the impulse response function analysis spanning a decade reveals no substantial impact, which could be attributed to several factors. Primarily, the lack of a significant response might suggest that South Africa's energy sector is robust against the climatic fluctuations associated with El Niño, potentially due to a varied energy portfolio or successful adaptive measures. Additionally, the graph's depiction could be indicative of economic mitigating elements that counterbalance the anticipated rise in energy consumption, including advancements in energy efficiency and consumer behavioral adjustments. The majority of IRF results associated with El Niño are depicted in Fig. 4. To maintain clarity and avoid visual congestion, the IRF outputs related to other countries are included in Fig. 6, which can be found in the appendix.

4.2. The La Niña effects

As previously mentioned, we administered a one standard deviation positive shock to the NEGBEST variable within our model to ascertain the impact of La Niña on energy consumption per capita across 26 country-specific models, spanning from the second quarter of 1979 to the third quarter of 2023. The outcomes of this analysis are graphically represented in Fig. 5. However, to enhance clarity and avoid visual congestion, the remaining impulse response function (IRF) can be found in the appendix, specifically inFig. 7. To briefly address the influence of La Niña on energy consumption per capita, we refrain from an exhaustive exposition. Instead, we direct attention to the synthesized results presented in Table 3, which encapsulate the essential findings without superfluous detail. It is noteworthy that previous studies have suggested that the La Niña phase exerts a considerably weaker influence than the El Niño phase across various aspects [26,32]. However, our findings contradict this notion, as La Niña has a significant effect on energy sectors in certain countries. This effect may be attributed to the changing nature of ENSO as global temperatures rise, leading to a stronger ENSO [44].

The elucidated patterns of energy consumption during the ENSO cycle, encompassing both El Niño and La Niña phenomena, hold profound implications for energy policy formulation. The discerned variability in energy demand underscores the necessity for adaptive policy frameworks that can accommodate the oscillating energy requirements precipitated by these climatic events. Policymakers are thus impelled to devise strategies that ensure energy supply resilience, promote energy diversification, and encourage the implementation of conservation measures during periods of climatic extremes. Furthermore, the insights gleaned from this study advocate for the integration of climate forecasting into energy planning, enabling preemptive adjustments to energy management and infrastructure investment decisions. Collectively, these measures are pivotal in fortifying the energy sector against the vicissitudes of the ENSO cycle, thereby safeguarding economic stability and environmental sustainability.

5. Conclusion and policy implications

This study delves into the impact of ENSO events on energy consumption per capita across 26 countries/regions. Leveraging the Global Vector Autoregressive (GVAR) model, we rigorously analyze the dynamic relationships between ENSO shocks and energy consumption patterns. Our empirical investigation sheds light on the diverse responses exhibited by different nations during El Niño and La Niña episodes, providing valuable insights for policymakers and energy stakeholders. By employing a comprehensive multi-country framework, we contribute substantively to the discourse on climate-energy interactions and advocate for evidence-based policy measures. Our impulse response analysis, grounded in empirical observations, reveals discernible patterns that inform critical decision-making in the context of energy resilience and sustainability. An increase in energy consumption per capita due to ENSO events is generally perceived as a negative effect because it underscores the heightened demand for energy to cope with adverse weather conditions. This increase leads to economic, environmental, and energy security challenges. El Niño adversely affects Australia, Indonesia, Malaysia, China, Japan, the USA, and Saudi Arabia. Conversely, La Niña has a positive impact on many more countries, including Argentina, Brazil, Chile, India, Mexico, and South Africa. The European region experiences a positive but insignificant impact during both El Niño and La Niña.

In addition to our empirical findings, we propose several policy implications to address the impact of ENSO events on energy consumption. Firstly, for countries vulnerable to El Niño (e.g., Australia, Indonesia, Malaysia), diversifying energy sources by investing in renewables can mitigate fossil fuel dependence during these events. Secondly, establishing strategic energy reserves helps buffer against supply disruptions caused by ENSO-related impacts. Thirdly, robust early warning systems are essential to anticipate El Niño events and their effects on energy markets. Additionally, during El Niño periods, demand-side management programs and smart grid technologies can enhance energy efficiency. Furthermore, fostering regional cooperation and joint contingency planning can mitigate energy disruptions. Finally, climate adaptation strategies, including implementing infrastructure and agricultural practices that are resilient to ENSO-induced weather variability, can be a crucial step in controlling GDP fluctuations. while our study provides valuable insights, certain variables (energy intensity, renewable energy share, carbon footprint, and energy efficiency metrics) were beyond our research scope due to data limitations. Future investigations could explore the impact of other climate oscillations (e.g., NAO,[9] PDO,[10] IOD,[11] MJO[12]) on energy consumption patterns. Moreover, our model excludes atmospheric variables such as temperature, precipitation, and humidity. In the GVAR model, we evaluate the coefficients in a large matrix. Given that the coefficients are estimated in very large matrices, the channels through which variables affect each other are not separately and distinctly identified.

Ethical approval

This article does not contain any studies with human participants or animals performed by any of the authors.

Funding

This research received no specific grant from any funding agency in the public, commercial, or not-for-profit sectors.

[9] North Atlantic Oscillation
[10] Pacific Decadal Oscillation
[11] Indian Ocean Dipole
[12] Madden-Julian Oscillation

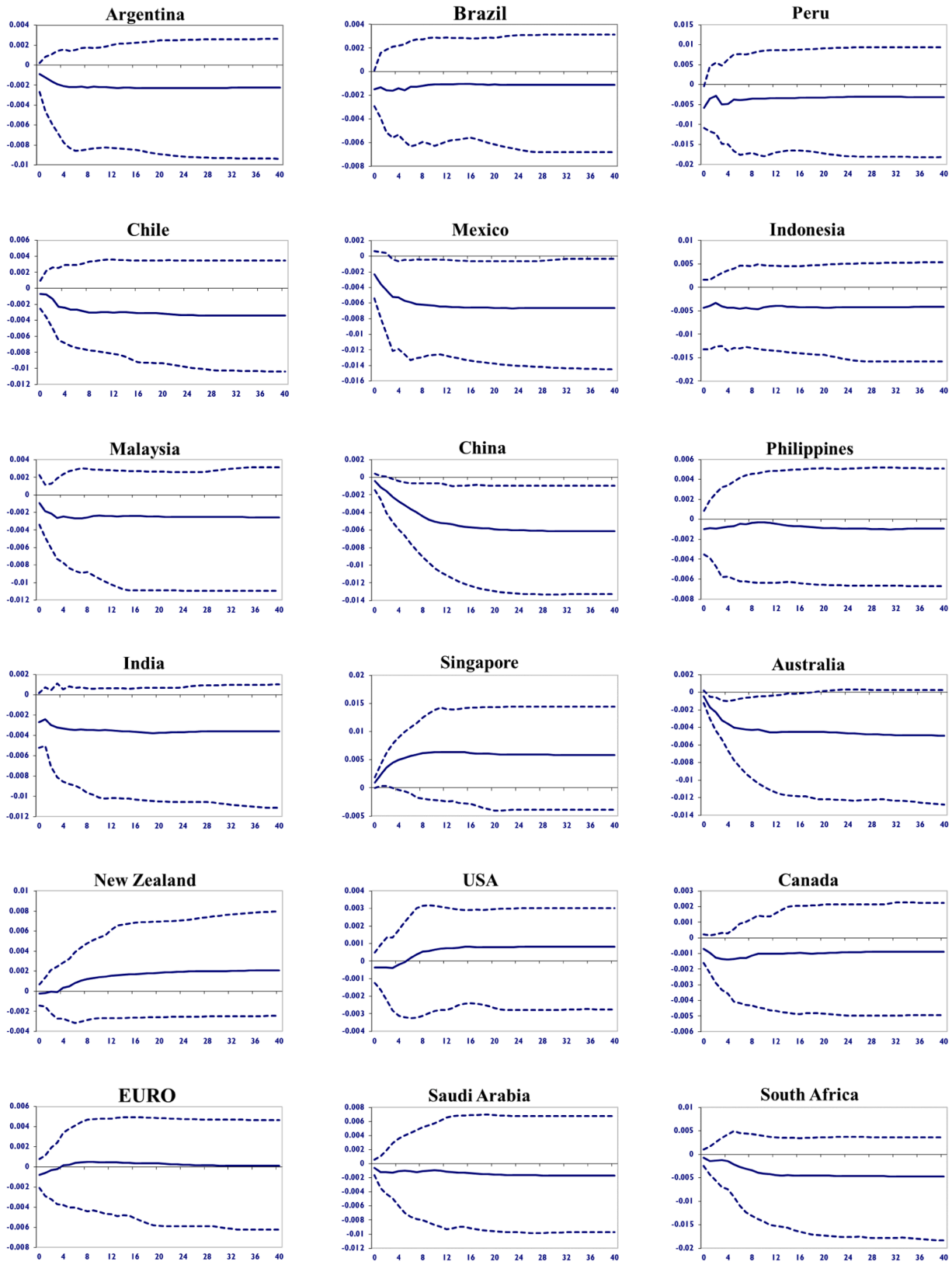

Fig. 5. The effects of a La Niña shock on energy consumption per capita. Notes: The figures represent the median impulse responses resulting from a one standard deviation positive shock to the negative component of BEST (NEGBEST). These responses are accompanied by the 5 %–95 % error bands (indicated by blue short-dashed lines), and the analysis is conducted at a quarterly horizon.

CRediT authorship contribution statement

Alireza Olfati: Writing – review & editing, Writing – original draft, Software, Methodology, Investigation, Formal analysis, Data curation. **Meysam Rafei:** Supervision, Software, Methodology, Conceptualization. **Siab Mamipour:** Writing – review & editing, Validation, Investigation, Formal analysis, Conceptualization.

Declaration of competing interest

The authors declare that they have no known competing financial interests or personal relationships that could have appeared to influence the work reported in this paper.

Appendix A

The rest of the impulse response functions separately for El Niño and La Niña are as follows:

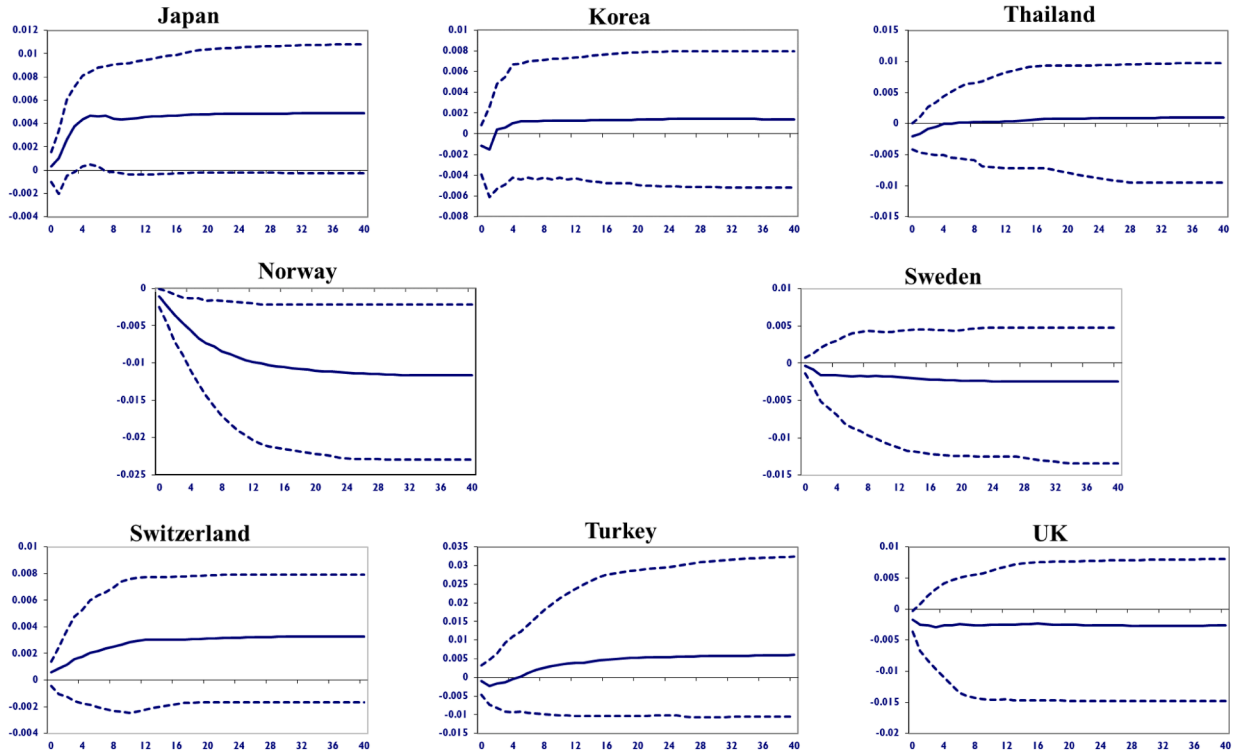

Fig. 6. The effects of an El Niño shock on energy consumption per capita. Notes: The figures represent the median impulse responses resulting from a one standard deviation negative shock to the positive component of BEST (POSBEST). These responses are accompanied by the 5 %–95 % error bands (indicated by blue short-dashed lines), and the analysis is conducted at a quarterly horizon.

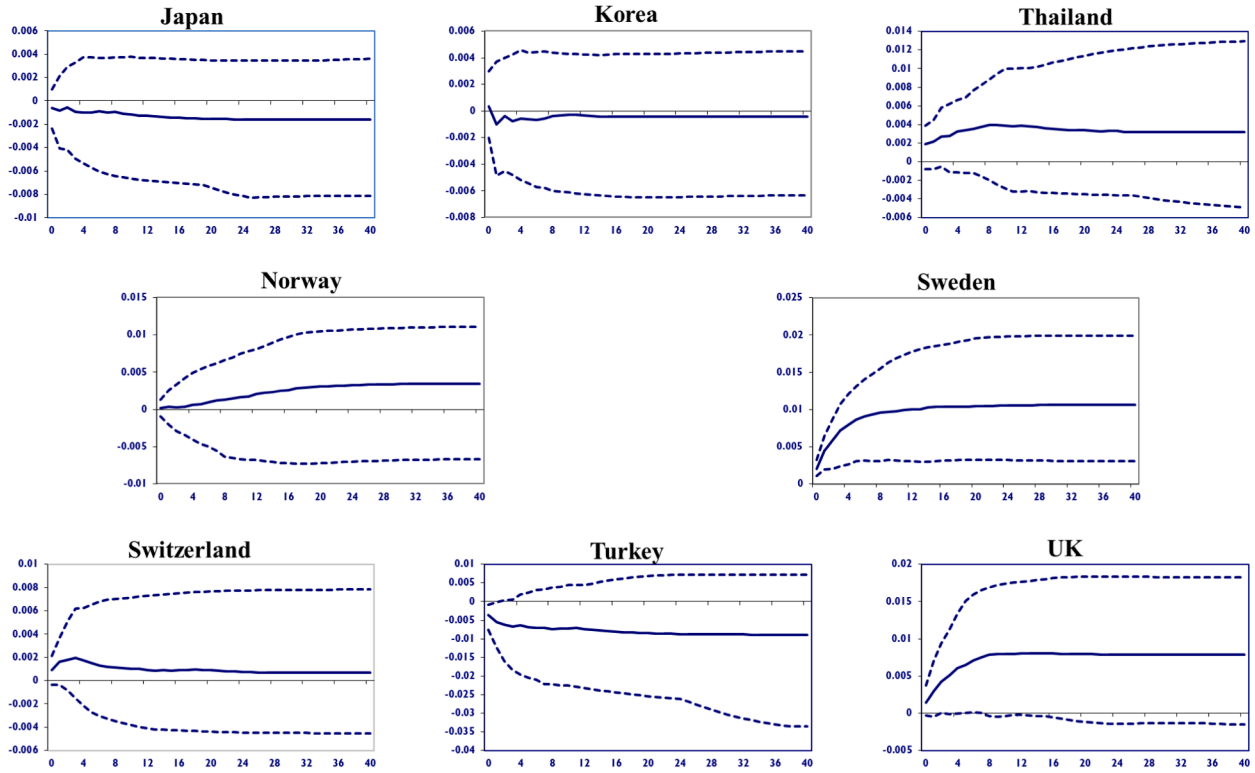

Fig. 7. The effects of a La Niña shock on energy consumption per capita. Notes: The figures represent the median impulse responses resulting from a one standard deviation positive shock to the negative component of BEST (NEGBEST). These responses are accompanied by the 5 %–95 % error bands (indicated by blue short-dashed lines), and the analysis is conducted at a quarterly horizon.

Appendix B[13]

ENSO events are characterized by significant Sea Surface Temperature (SST) anomalies in the tropical Pacific, which influence global atmospheric circulation patterns, such as the jet stream and Hadley circulation. For example, during El Niño, the jet stream often shifts southward, bringing increased precipitation to some regions and causing droughts in others. ENSO events also cause temperature anomalies and changes in precipitation and wind patterns that affect energy consumption. During El Niño, higher temperatures in regions like North America and Europe increase the demand for cooling energy. Conversely, La Niña can lead to lower temperatures and higher heating energy demand.

In this part, we focus on the relationship between temperature changes and El Niño/La Niña, as shown by the BEST index in Fig. 8**.** As is well-documented, the years 1982–83, 1997–98, and 2015–16 experienced severe El Niño events. During these El Niño years, temperatures significantly increased in Australia, located in the Southern Hemisphere. In 2015, the weather was notably warm, with both maximum and minimum temperatures being much above average for most of the country. It was the warmest October on record for the nation as a whole. A meticulous examination of Fig. 8 reveals a clear relationship between temperature changes and El Niño years.

Consequently, the hotter summers experienced in Australia during these periods led to an increase in energy consumption. This increase in energy consumption during the mentioned years is also evident in countries like Indonesia and Malaysia, where temperatures significantly rise. Conversely, Argentina experiences relatively milder summers due to increased rainfall, resulting in decreased temperatures during El Niño years. Hence, a reduction in energy consumption is expected during the summers in Argentina, Brazil, and even Peru, as clearly illustrated in Fig. 9**.**

We used the Hodrick-Prescott Filter to analyze the cycles of energy consumption per capita for each country and compare them with the cycles of the BEST Index (refer to Fig. 9). It is important to note that, due to economic frictions, there can sometimes be a lag in the observed variables. However, these graphs provide evidence supporting the results of our impulse response functions.

[13] All data, including energy consumption per capita, temperature changes, and the BEST Index, along with all graphs for each country separately, can be provided upon request.

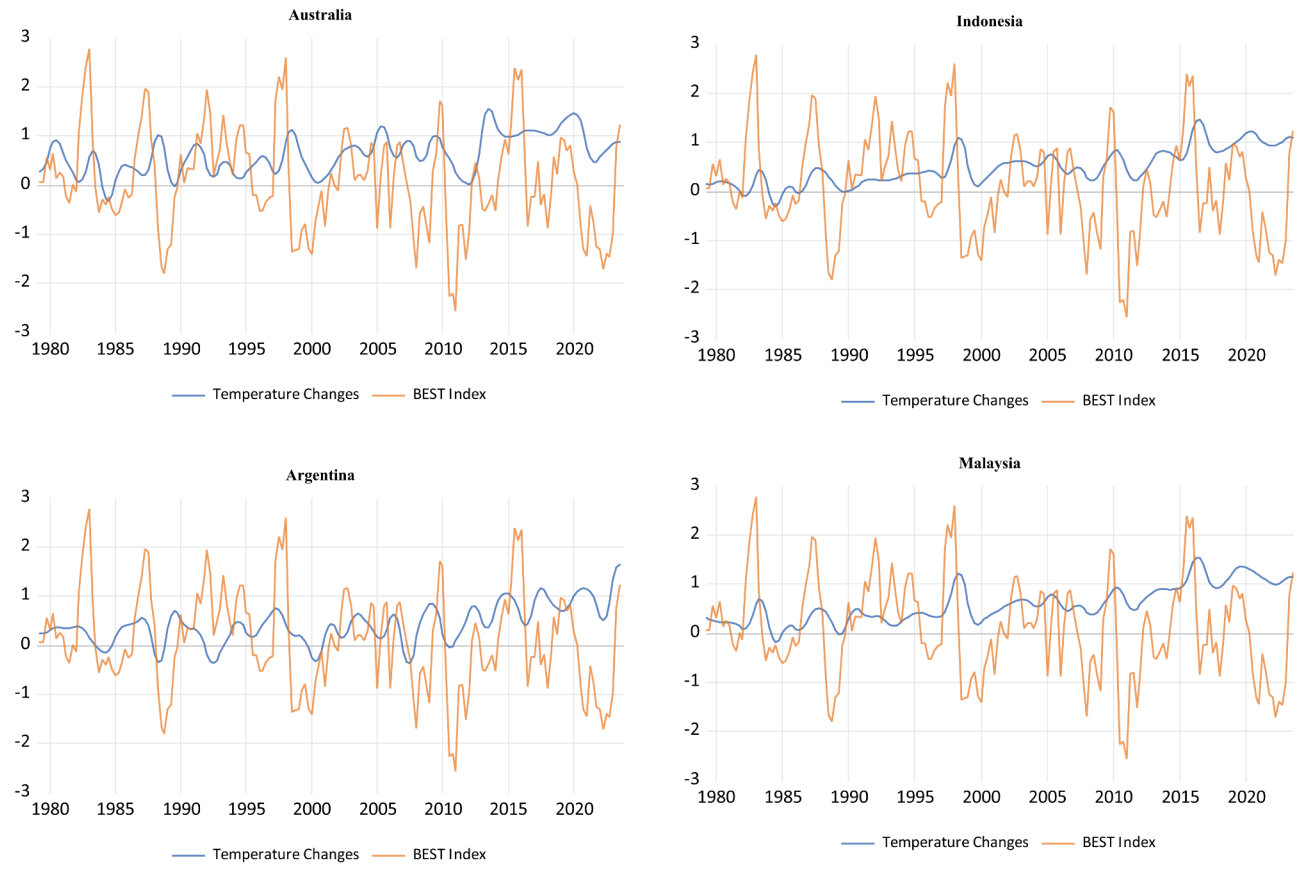

Fig. 8. Relationship between the best index as an indicator for El Niño and La Niña, and temperature changes for four countries that are among the most affected by ENSO events.

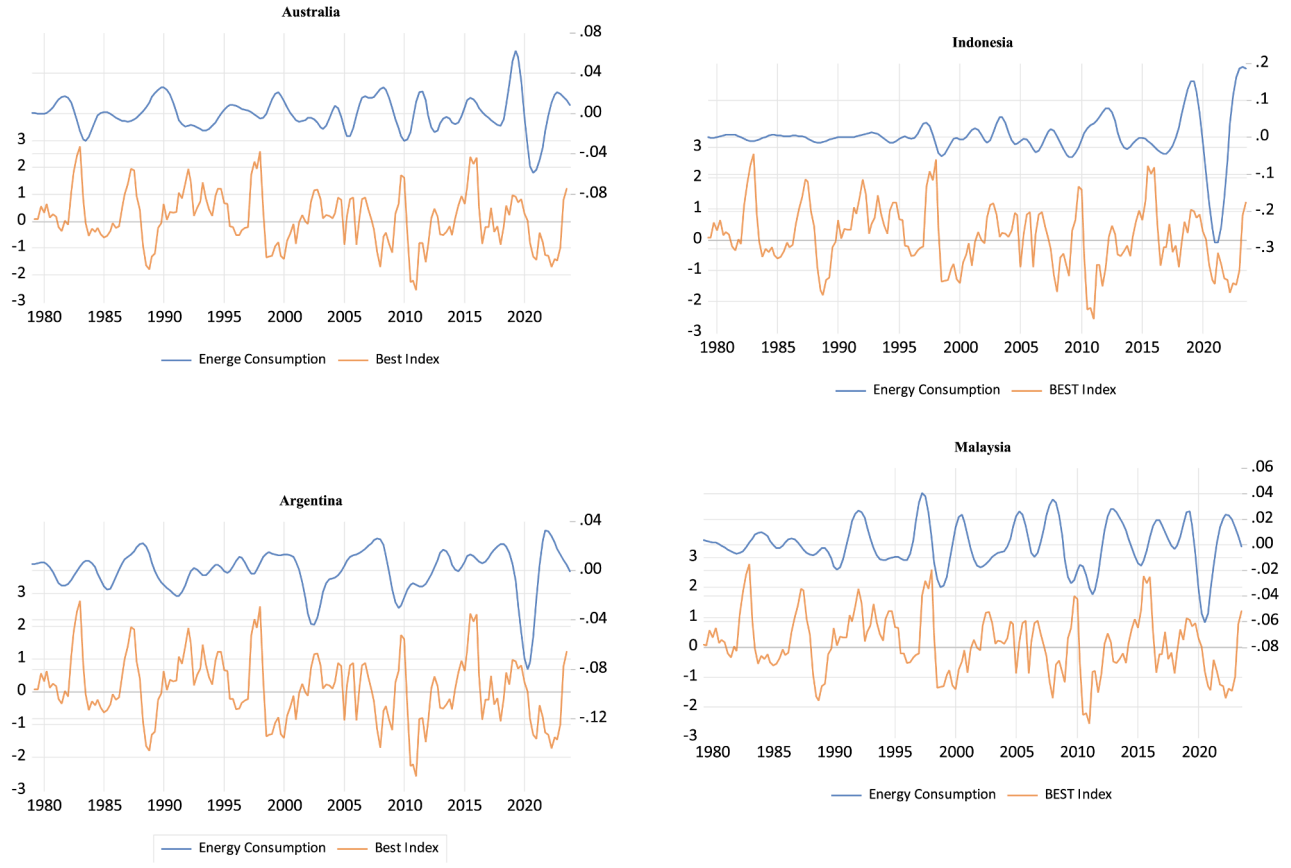

Fig. 9. Relationship between the best index as an indicator for El Niño and La Niña, and energy consumption per capita for four countries that are among the most affected by ENSO event.

Data availability

Data will be made available on request.

References

[1] N. Antonakakis, I. Chatziantoniou, G. Filis, Energy consumption, CO 2 emissions, and economic growth: an ethical dilemma, Renew. Sustain. Energy Rev. 68 (2017) 808–824, https://doi.org/10.1016/j.rser.2016.09.105.

[2] M.H. Azmoodehfar, S.A. Azarmsa, Assessment the effect of ENSO on weather temperature changes using fuzzy analysis (case study: chabahar), APCBEE Procedia 5 (2013) 508–513.

[3] W. Cai, M.J. McPhaden, A.M. Grimm, R.R. Rodrigues, A.S. Taschetto, R. D. Garreaud, B. Dewitte, G. Poveda, Y.G. Ham, A. Santoso, Climate impacts of the El Niño–southern oscillation on South America, Nat. Rev. Earth. Environ. 1 (4) (2020) 215–231.

[4] W. Cai, M.J. McPhaden, A.M. Grimm, R.R. Rodrigues, A.S. Taschetto, R. D. Garreaud, B. Dewitte, G. Poveda, Y.G. Ham, A. Santoso, B. Ng, W. Anderson, G. Wang, T. Geng, H.S. Jo, J.A. Marengo, L.M. Alves, M. Osman, S. Li, C. Vera, Climate impacts of the El Niño–Southern Oscillation on South America, Nat. Rev. Earth. Environ. 1 (4) (2020) 215–231, https://doi.org/10.1038/s43017-020-0040-3.

[5] A. Calzadilla, K. Rehdanz, R. Betts, P. Falloon, A. Wiltshire, R.S. Tol, Climate change impacts on global agriculture, Clim. Change 120 (2013) 357–374.

[6] A. Capotondi, A.T. Wittenberg, M. Newman, E. Di Lorenzo, J.Y. Yu, P. Braconnot, J. Cole, B. Dewitte, B. Giese, E. Guilyardi, Understanding ENSO diversity, Bull. Am. Meteorol. Soc. 96 (6) (2015) 921–938.

[7] P. Cashin, K. Mohaddes, M. Raissi, Fair weather or foul? The macroeconomic effects of El Niño, J. Int. Econ. 106 (2017) 37–54, https://doi.org/10.1016/j.jinteco.2017.01.010.

[8] A. Chudik, M.H. Pesaran, Econometric analysis of high dimensional VARs featuring a dominant unit, Econ. Rev. 32 (5–6) (2013) 592–649.

[9] A. Chudik, M.H. Pesaran, Theory and practice of GVAR modelling, J. Econ. Surv. 30 (1) (2016) 165–197.

[10] K.J. Collins, How El Nino Affects Energy consumption: a Study At National and Regional Levels, Texas A & M University, 2010.].

[11] S. Dees, F.d. Mauro, M.H. Pesaran, L.V. Smith, Exploring the international linkages of the euro area: a global VAR analysis, J. Appl. Econom. 22 (1) (2007) 1–38.

[12] M. Dell, B.F. Jones, B.A. Olken, What do we learn from the weather? The new climate-economy literature, J. Econ. Lit. 52 (3) (2014) 740–798.

[13] R. Demirer, R. Gupta, J. Nel, C. Pierdzioch, Effect of rare disaster risks on crude oil: evidence from El Niño from over 145 years of data, Theor. Appl. Clim. 147 (1–2) (2021) 691–699, https://doi.org/10.1007/s00704-021-03856-x.

[14] R. Emberson, D. Kirschbaum, T. Stanley, Global connections between El Nino and landslide impacts, Nat. Commun. 12 (1) (2021) 2262, https://doi.org/10.1038/s41467-021-22398-4.

[15] R. Emberson, D. Kirschbaum, T. Stanley, Global connections between El Nino and landslide impacts, Nat. Commun. 12 (1) (2021) 2262.

[16] W. Ginn, Does ENSO impact equity returns? Evidence via country and panel regression, Int. Econ. J. 38 (2024) 345–364, https://doi.org/10.1080/10168737.2024.2320116.

[17] M.H. Glantz, Currents Of Change: Impacts of El Niño and La Niña On Climate and Society, Cambridge University Press, 2001.

[18] C. Gong, C. Xu, Influence of air quality ranking on China's energy efficiency: spatial difference-in-differences model with multiple time periods, Environ. Sci. Pollut. Res. 30 (12) (2023) 34573–34584.

[19] L. Gutierrez, Impacts of El Nino-Southern Oscillation on the wheat market: a global dynamic analysis, PLoS. One 12 (6) (2017) e0179086, https://doi.org/10.1371/journal.pone.0179086.

[20] M. Holmgren, M. Scheffer, E. Ezcurra, J.R. Gutiérrez, G.M. Mohren, El Niño effects on the dynamics of terrestrial ecosystems, Trends Ecol. Evol. 16 (2) (2001) 89–94.

[21] S.M. Hsiang, K.C. Meng, M.A. Cane, Civil conflicts are associated with the global climate, Nature 476 (7361) (2011) 438–441.

[22] H.Y. Kao, J.Y. Yu, Contrasting eastern-Pacific and central-Pacific types of ENSO, J. Clim. 22 (3) (2009) 615–632.

[23] K.C. Lee, M.H. Pesaran, Persistence profiles and business cycle fluctuations in a disaggregated model of UK output growth, Ric. Econ. 47 (3) (1993) 293–322.

[24] J. Lin, T. Qian, A new picture of the global impacts of El Nino-southern oscillation, Sci. Rep. 9 (1) (2019) 17543, https://doi.org/10.1038/s41598-019-54090-5.

[25] R.B. Litterman, Forecasting with Bayesian vector autoregressions—five years of experience, J. Bus. Econ. Stat. 4 (1) (1986) 25–38.

[26] Y. Liu, W. Cai, X. Lin, Z. Li, Y. Zhang, Nonlinear El Nino impacts on the global economy under climate change, Nat. Commun. 14 (1) (2023) 5887, https://doi.org/10.1038/s41467-023-41551-9.

[27] M.J. McPhaden, S.E. Zebiak, M.H. Glantz, ENSO as an integrating concept in earth science, Science 314 (5806) (2006) 1740–1745.
[28] M.H. Pesaran, General diagnostic tests for cross section dependence in panels. Cambridge working papers, Economics 1240 (1) (2004) 1.
[29] M.H. Pesaran, Y. Shin, Cointegration and speed of convergence to equilibrium, J. Econ. 71 (1–2) (1996) 117–143.
[30] M.H. Pesaran, Y. Shin, R.J. Smith, Structural analysis of vector error correction models with exogenous I (1) variables, J. Econ. 97 (2) (2000) 293–343.
[31] S. Power, F. Delage, C. Chung, G. Kociuba, K. Keay, Robust twenty-first-century projections of El Niño and related precipitation variability, Nature 502 (7472) (2013) 541–545.
[32] A.A. Salisu, R. Gupta, J. Nel, E. Bouri, The (Asymmetric) effect of El Niño and La Niña on gold and silver prices in a GVAR model, Resour. Policy. (2022) 78, https://doi.org/10.1016/j.resourpol.2022.102897.
[33] C.A. Smith, P.D. Sardeshmukh, The effect of ENSO on the intraseasonal variance of surface temperatures in winter, J. R. Meteorol. Soc. 20 (13) (2000) 1543–1557.
[34] L.V. Smith, A. Galesi, GVAR Toolbox 2.0, University of Cambridge: Judge Business School, 2014.
[35] K. Thakker, R.S. Teegavarapu, Evaluation of influences of ENSO events on changes in temperature extremes and energy consumption in South Florida, World Environ. Water Resour. Congr. (2020) 2020.
[36] A. Timmermann, S.I. An, J.S. Kug, F.F. Jin, W. Cai, A. Capotondi, K.M. Cobb, M. Lengaigne, M.J. McPhaden, M.F. Stuecker, El Niño–southern oscillation complexity, Nature 559 (7715) (2018) 535–545.
[37] R.S.J. Tol, The economic effects of climate change, J. Econ. Perspect. 23 (2) (2009) 29–51.
[38] D. Ubilava, M. Abdolrahimi, The El Niño impact on maize yields is amplified in lower income teleconnected countries, Environ. Res. Lett. 14 (5) (2019), https://doi.org/10.1088/1748-9326/ab0cd0.
[39] Y. Wei, J. Zhang, L. Bai, Y. Wang, Connectedness among El Niño-Southern Oscillation, carbon emission allowance, crude oil and renewable energy stock markets: time- and frequency-domain evidence based on TVP-VAR model, Renew. Energy 202 (2023) 289–309, https://doi.org/10.1016/j.renene.2022.11.098.
[40] Y. Wei, J. Zhang, Y. Chen, Y. Wang, The impacts of El Niño-southern oscillation on renewable energy stock markets: evidence from quantile perspective, Energy (2022) 260, https://doi.org/10.1016/j.energy.2022.124949.
[41] N. Wen, L. Li, J.J. Luo, Direct impacts of different types of El Niño in developing summer on East Asian precipitation, Clim. Dyn. 55 (5–6) (2020) 1087–1104, https://doi.org/10.1007/s00382-020-05315-1.
[42] N. Wen, L. Li, J.J. Luo, Direct impacts of different types of El Niño in developing summer on East Asian precipitation, Clim. Dyn. 55 (5) (2020) 1087–1104.
[43] T. Wheeler, J. Von Braun, Climate change impacts on global food security, Science 341 (6145) (2013) 508–513.
[44] S. Yang, Z. Li, J.Y. Yu, X. Hu, W. Dong, S. He, El Niño–Southern Oscillation and its impact in the changing climate, Natl. Sci. Rev. 5 (6) (2018) 840–857.
[45] J.Y. Yu, H.Y. Kao, Decadal changes of ENSO persistence barrier in SST and ocean heat content indices: 1958–2001, J. Geophys. Res.: Atmos. 112 (D13) (2007).
[46] L. Zeng, Y. Yang, H. Wang, J. Wang, J. Li, L. Ren, H. Li, Y. Zhou, P. Wang, H. Liao, Intensified modulation of winter aerosol pollution in China by El Niño with short duration, Atmos. Chem. Phys. 21 (13) (2021) 10745–10761.
[47] L. Zhang, Y. Li, S. Yu, L. Wang, Risk transmission of El Niño-induced climate change to regional Green Economy Index, Econ. Anal. Policy. 79 (2023) 860–872, https://doi.org/10.1016/j.eap.2023.07.006.